Remote Sens. **2013**, *5*, 4280-4303; doi:10.3390/rs5094280

OPEN ACCESS

Remote Sensing

ISSN 2072-4292

www.mdpi.com/journal/remotesensing

Article

Hub Height Ocean Winds over the North Sea Observed by the NORSEWInD Lidar Array: Measuring Techniques, Quality Control and Data Management

Charlotte Bay Hasager [1,*], Detlef Stein [2], Michael Courtney [1], Alfredo Peña [1], Torben Mikkelsen [1], Matthew Stickland [3] and Andrew Oldroyd [4]

[1] Department of Wind Energy, Technical University of Denmark, Frederiksborgvej 399, 4000 Roskilde, Denmark; E-Mails: mike@dtu.dk (M.C.); aldi@dtu.dk (A.P.); tomi@dtu.dk (T.M.)

[2] GL Garrad Hassan, Brooktorkai 18, D-20457 Hamburg, Germany; E-Mail: Detlef.stein@gl-group.com

[3] Department of Mechanical Engineering, University of Strathclyde, Glasgow G1 1XJ, UK; E-Mail: matt.stickland@strath.ac.uk

[4] Oldbaum Services, Stirling FK9 4NF, UK; E-Mail: andy@oldbaumservices.co.uk

* Author to whom correspondence should be addressed; E-Mail: cbha@dtu.dk; Tel.: +45-2132-7328; Fax: +45-4677-5970.

Received: 28 July 2013; in revised form: 3 September 2013 / Accepted: 3 September 2013 / Published: 5 September 2013

Abstract: In the North Sea, an array of wind profiling wind lidars were deployed mainly on offshore platforms. The purpose was to observe free stream winds at hub height. Eight lidars were validated prior to offshore deployment with observations from cup anemometers at 60, 80, 100 and 116 m on an onshore met mast situated in flat terrain. The so-called "NORSEWInD standard" for comparing lidar and mast wind data includes the criteria that the slope of the linear regression should lie within 0.98 and 1.01 and the linear correlation coefficient higher than 0.98 for the wind speed range 4–16 $m \cdot s^{-1}$. Five lidars performed excellently, two slightly failed the first criterion and one failed both. The lidars were operated offshore from six months to more than two years and observed in total 107 months of 10-min mean wind profile observations. Four lidars were re-evaluated post deployment with excellent results. The flow distortion around platforms was examined using wind tunnel experiments and computational fluid dynamics and it was found that at 100 m height wind observations by the lidars were not significantly influenced by flow distortion. Observations of the vertical wind profile shear exponent at hub height are presented.

Keywords: lidar; offshore winds; remote sensing; wind energy; wind resources

1. Introduction

There is need for accurate information on ocean winds for offshore wind farms and turbine clusters in the Northern European Seas. In large offshore wind farm projects the economic risk is considerably reduced when accurate wind data are available at hub height for a minimum of one year. For a decrease in uncertainty on the predicted mean wind speed at hub height of 0.1 $m \cdot s^{-1}$ there is an estimated saving worth around £10 million per year for 25 years for a large offshore wind farm project according to industry experts. The cost of installing and operating tall meteorological masts has increased in recent years and has a price tag around £10 million for a two-year campaign, thus alternatives are desirable.

The motivation for choosing lidar remote sensing technology is to provide ocean wind data at higher levels than meteorological masts' typical span and at the same time to ensure high accuracy wind speed measurements at relatively low cost. The need for improved knowledge on winds at higher levels is twofold: Firstly modern wind turbines, especially offshore, are increasing in dimension and the flow across their large rotors is not well-explained by hub height winds alone [1]. Secondly the marine atmospheric boundary layer and its temporal behavior at higher levels are poorly known. There is a need for improved parameterizations of the marine vertical wind profiles in order to improve modeling of offshore winds for wind energy [2] and to experimentally evaluate atmospheric wind resource model predictions against offshore winds [3].

Wind lidar remote sensing has had a very rapid growth and dissemination within the wind energy community in recent years. The early experiments at DTU Wind Energy (formerly Risø) with a focused continuous wave (cw) Doppler wind lidar took place onshore over flat terrain at Høvsøre near the tall meteorological mast in 2003 [4]. This was followed by an experimental deployment offshore on the Fino-1 platform in 2005 [5], the Nysted 1 offshore wind farm transformer platform in 2006 [6] and the Horns Rev 1 offshore wind farm transformer platform in 2007 [2]. At all three offshore sites meteorological masts were located nearby and the concurrent meteorological observations were used for comparisons to the lidar observations. The data analysis from these early offshore experiments gave promising results. This fact stimulated the idea for using an array of wind profiling lidars in the Northern European Seas where the majority of European offshore wind farms are planned but where the knowledge of the wind resources is limited.

In the EU FP7 Northern Sea Wind Index Database (NORSEWiND) investigation from 2008 to 2012 [7] nine lidars were deployed on offshore platforms in the North Sea and one lidar was deployed near the coast of the Norwegian island of Utsira. The research objectives of the NORSEWiND project included systematic analysis of the marine wind shear observed from the lidars [8] and investigation of the flow distortion around the offshore platforms [9]. It was important to investigate the platforms' influence on the free stream wind speed profiles at hub height. Other results from the project included a wind atlas based on numerical modeling and satellite data [3,10–15]. The wind atlas is public available from the project web-site.

The purpose of this article is to present the lessons learnt on the lidar measurement technique, deployment strategies and pre- and post- deployment validation including the definition of data quality acceptance levels: the so-called "NORSEWiND standard". Also the requirements for installation setup, the data availability, system consistency and multi-year performance are described. The work demonstrates the data management strategy for reliable application of lidar data. The measurement of flow distortion by the platforms using sub-scale models in a wind tunnel and computational fluid dynamics is described with the aim to clarify the level of flow distortion influence on the lidar wind profile observations at hub height. A total of 77.491 h, approximately 107 operational months of wind profile data from 10 lidars in the period July 2009 to April 2012 were recorded. The data are stored as 10-min values in a MySQL database. Selected results of the wind shear at hub height are presented and discussed.

2. The NORSEWInD Study Area

Nine lidars were deployed on offshore platforms. One lidar was deployed on the coast of the island of Utsira. Figure 1 illustrates the locations.

Figure 1. Map of lidar positions and the Høvsøre test site.

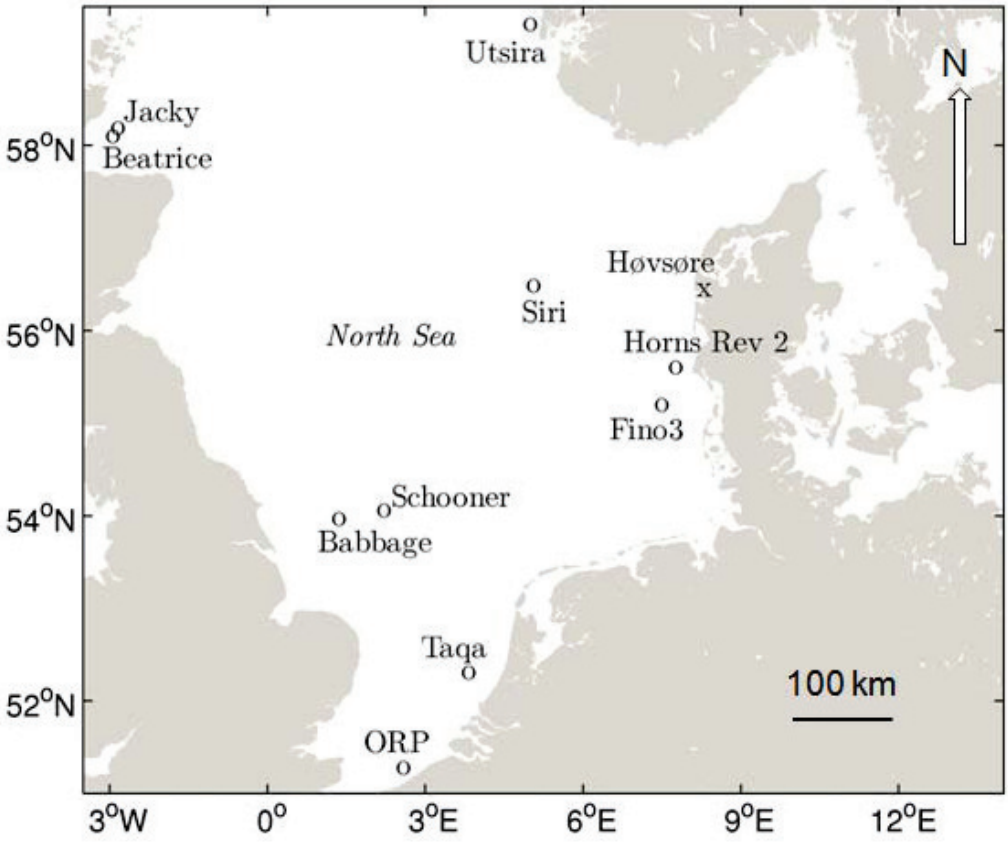

The lidars were operated on the platforms over the period from July 2009 to April 2012. Only during a short period in the summer of 2011 did all lidars but one operate simultaneously. An overview of the periods of operation is given in Figure 2. The reasons for the different start times and durations of observations were due to practical issues and logistics.

Figure 2. Overview of observation period from the lidars.

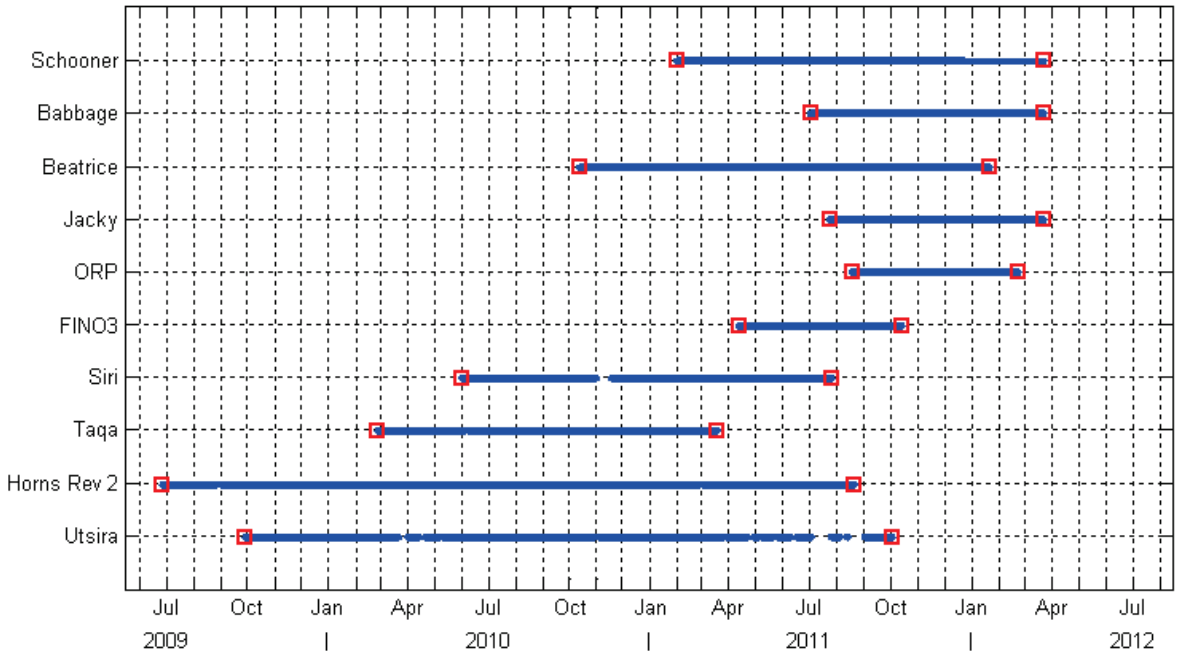

3. Deployment Strategies at Offshore Platforms

All lidars in the NORSEWiND project were planned to provide stand-alone wind profile observations offshore over many months of operation, *i.e.*, there would not be nearby meteorological masts for comparison during the offshore deployment. This prompted a need for careful pre- and post-deployment validations. Access to the lidars at the offshore platforms is limited thus it was necessary to plan carefully.

The lidars were selected by the industrial partners and encompassed focused cw Doppler wind lidars of the type ZephIR® [16,17] and pulsed wind lidars of the type WindCubeWLS7® [18,19]. Dependent upon the height of the platform at which each lidar would be installed there were specific deployment plans for the two types of lidars. The key aim was to observe wind profiles without significant flow distortion from the platforms and to observe winds at several heights in free stream conditions. It was decided as most important to observe winds at 100 m above mean sea level (AMSL) as it is expected to be close to the hub heights of future offshore wind turbines. A wind turbine with a rotor diameter of 120 m will sweep from 40 to 160 m AMSL. The wind profiles were planned to be observed within these height ranges in steps of 20 m, typically at 5 or 6 heights for the ZephIRs and at 10 heights for the WindCubes.

The deployment requirements for each platform or rig included technical and legal considerations. From the technical perspective it was important to clarify the access to the platform and to ensure the installation would be at a suitable location with a level and vibration-free position and the mounting would be with free view for all laser beam directions. The free view may potentially be disturbed by the rig, cranes, derricks, building, *etc*. As an example Figure 3 shows photographs of some lidars in situ to demonstrate the selected installation spots. On oil and gas rigs the installation location was selected to be as far as possible from exhausts and flares. It was important to avoid high aerosol

concentrations that could either corrupt the measured wind speed or cause complete extinction of the laser light and thus prevent valid measurements.

Figure 3. Photograph of selected lidars on platform.

The lidars need a power supply and a communication network. Thus it was important to ensure a suitable and uninterrupted power supply and to check if un-regulated or un-buffered power supply could occur. Furthermore, the communication network was required to allow remote control, data retrieval access and time synchronization. At some platforms cable line was hooked up at Ethernet and using VPN. The time synchronization was important since the internal clocks of unattended lidars may significantly drift if they are not actively synchronized (there were unfortunately examples of this). The drift is typically around one to three seconds per day; thus it needs update once per day or hour. A network time server (if available) or an onboard Global Positioning System (GPS) device can be used as reference time sources. NTP protocol was used once per day typically. On offshore platforms debris from birds is common. This should not fall on the lidar's optical port. Therefore spikes or cages were established. Large amounts of the wiper fluids were provided and connected to keep the lidar windows/lenses clean. The wash and wipe systems were regularly revisited.

On the un-manned platforms theft protection was carried out. At manned platforms/rigs the personnel were instructed to perform operation and maintenance of the remote sensing instruments. In fact, it proved very important that this instruction/training was carefully undertaken to allow best operation of lidars. After installation a thorough on-site test was done. The systems were configured for immediate safe shutdown.

4. Deployment Validation Strategies

As already stated, the lidars were planned to operate stand-alone offshore for many months. This prompted a need for pre- and post-deployment validations. Thus the NORSEWInD deployment validation strategies included three major steps: Pre-deployment validation onshore, data collection and operational performance validation at sea, and post-deployment validation onshore.

The pre- and post-deployment validations onshore took place at the DTU Wind Energy's Høvsøre test site on the Danish North Sea coast next to a 116 m tall meteorological mast on flat terrain. The observations from the lidars were compared to the mast observations at the levels 60, 80, 100 and 116 m. The local set up arrangement is shown in Figure 4.

Figure 4. Høvsøre mast and lidar set up sketch.

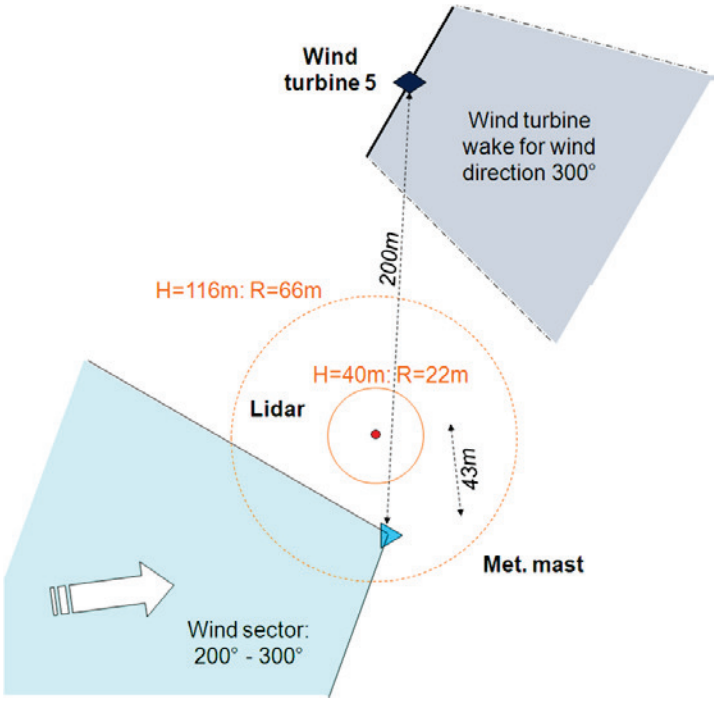

Prior to the pre-deployment validation a standard for the data quality acceptance levels for the NORSEWInD lidar systems was defined. This is the so-called "NORSEWInD standard" and the details are given in Table 1.

The pre-deployment validation included eight lidars. Figure 5 shows the comparison results between observed wind speeds from cup anemometer and lidar measurements at 100 m for one of the lidars. The observations are from the wind sector 200° to 300° at Høvsøre (see the sector in Figure 4). The linear regression slope and R^2 at all observational heights for the eight lidars tested for $y = mx$ are listed in Table 2. Only three instruments (1, 7 and 9) did not fully pass the criteria. The poorer values are highlighted in grey. The results of the verification for these systems may be seen to be only slightly out of range except for the measurement at 60 m by Lidar 1. Lidars 1 to 5 are WindCubes. Lidars 6 to 8 are ZephIRs. The pre-deployment validation showed excellent results for most of the lidars deployed. The slopes and correlation coefficients are slightly lower for the Zephirs than WindCubes except for Lidar 1. The reason may be due to comparison between point data from the mast to line scanning from pulsed lidars (WindCube) and volume scanning (Zephirs) from remote sensing data.

Table 1. Data quality acceptance levels for NORSEWInD lidar systems. *u* stands for wind speed.

Parameter	Criteria	Ranges (Height and Speed)
Absolute error	<0.5 m·s^{-1} for 2 < *u* < 16 m·s^{-1} Within 5% above 16 m·s^{-1} Not more than 10% of data to exceed those values	All valid data
Data availability	Assessed case by case Environmental conditions dependency	All valid data
Linear regression Slope	Slope between 0.98 and 1.01 <0.015 variation in slope between *u*-ranges (b) and (c)	Heights from 60 to 116 m *u*-ranges: (a) 4–16 m·s^{-1}, (b) 4–8 m·s^{-1}, (c) 8–12 m·s^{-1}
Linear regression Correlation coefficent (R^2)	>0.98	Heights from 60 to 116m *u*-ranges: (a) 4–16 m·s^{-1}, (b) 4–8 m·s^{-1}, (c) 8–12 m·s^{-1}

Figure 5. Wind speed observed from cup anemometer and WindCube lidar at 100 m at Høvsøre. The vertical lines indicate the 4, 8 and 12 m·s^{-1} levels.

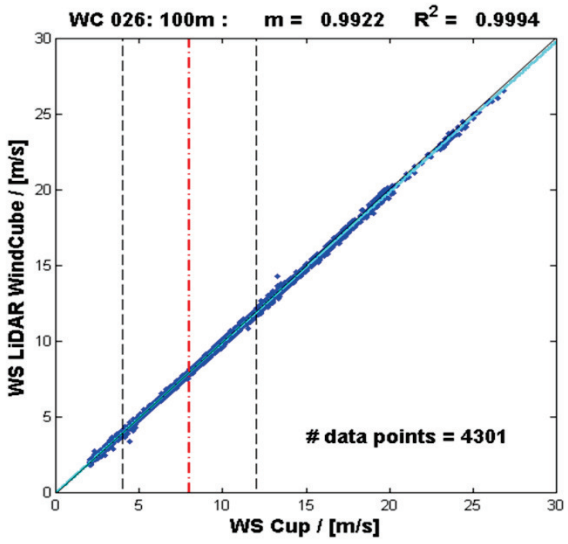

Table 2. Pre-deployment validation results shown for eight lidars tested at Høvsøre: Linear correlation slope and R^2 for the wind speeds in the range from 4 to 16 m·s^{-1} at four heights.

Lidar	Slope at				R^2 at			
	116 m	100 m	80 m	60 m	116 m	100 m	80 m	60 m
1	0.991	0.976	0.977	0.948	0.999	0.976	0.974	0.915
2	0.988	0.992	0.991	0.993	0.999	0.999	0.998	0.998
3	0.993	0.997	0.997	1.000	0.998	0.998	0.998	0.997
4	0.996	0.999	0.998	0.998	0.999	0.999	0.999	0.998
5	0.985	0.993	0.992	0.993	0.999	0.998	0.998	0.997
6	0.983	0.986	0.986	0.990	0.996	0.996	0.996	0.995
7	0.978	0.983	0.984	0.992	0.994	0.994	0.995	0.995
8	0.976	0.980	0.977	0.989	0.995	0.996	0.996	0.995

The post-deployment validation only included four out of the eight pre-deployment validated lidars. The post-deployment was done at the same location. The instruments at the mast had been changed due to normal maintenance of the high-quality instruments. The observational levels were the same as for the pre-deployment validation. Thus the NORSEWInD post-deployment performance consistency check is assumed to provide reliable statistics on the multi-year performances of the lidars. Table 3 shows the pre- and post-deployment validation results.

Table 3. Pre-and post-deployment validation results and the differences (diff.) are shown for the four lidars tested at Høvsøre (DTU Wind Energy): Linear correlation slope and R^2 for the wind speeds in the range from 4 to 16 $m \cdot s^{-1}$ at four heights. The number of 10-min observation (N) is given.

Lidar	Time	Slope at				R^2 at				N
		116 m	100 m	80 m	60 m	116 m	100 m	80 m	60 m	
	Pre	0.988	0.992	0.991	0.993	0.999	0.999	0.998	0.998	3.606
2	Post	0.991	0.997	0.993	0.992	0.999	0.998	0.998	0.997	3.659
	Diff.	0.003	0.005	0.002	−0.001	0.000	−0.001	0.000	−0.001	-
	Pre	0.996	0.999	0.998	0.998	0.999	0.999	0.999	0.998	5.065
4	Post	0.989	0.994	0.989	0.999	0.998	0.998	0.998	0.997	3.510
	Diff.	−0.007	−0.005	−0.009	0.001	−0.001	−0.001	−0.001	−0.001	-
	Pre	0.985	0.993	0.992	0.993	0.999	0.998	0.998	0.997	991
5	Post	0.983	0.987	0.984	0.992	0.999	0.999	0.998	0.998	2.791
	Diff.	−0.002	−0.005	−0.008	−0.001	0.000	0.000	0.001	0.001	-
	Pre	0.976	0.980	0.977	0.989	0.995	0.996	0.996	0.995	1.547
8	Post	0.960	0.971	0.970	0.979	0.993	0.994	0.995	0.995	1.206
	Diff.	−0.016	−0.009	−0.007	−0.010	−0.002	−0.002	−0.001	0.000	-

The post-deployment validation statistics are similar to the pre-deployment validation to the second decimal except for Lidar 9 at 116 m. This consistency check on the lidar's performance shows instruments with a high degree of repeatability and able to endure from several months to two years deployment on the offshore platforms. This is a comforting result as the aim of the NORSEWInD experimental campaign was to observe offshore winds with high accuracy over an extended period of time.

5. Data Collection and Operational Performance Validation at Sea

The lidars were mounted on nine offshore platforms and the island of Utsira. In Table 4 the height of the instrument mounting on the platforms and observational heights are listed in meters AMSL. The observational heights at or near 100 m are shown in italic type in Table 4. These heights are, for simplicity, described as at around 100 m hereafter. The ten lidars were deployed for a total of 91.603 h. For the 77.491 h of data the average data availability was 89%.

The system and data availability at around 100 m for the lidars is provided in Table 5. The system availability is defined as the time from the mounting to dismounting of the lidar. The downtime in system availability was due to different reasons. One was a mechanical failure of the rotation of lens/mirror in one instrument. In other cases the wiper motors and assembly had problems. They were

re-fitted when possible. The data availability is defined as the instrument is operational but may not (fully) observe data. One reason was that the wiper spraying was working fine but for some instruments the back and forth movement of the wiper caused sometimes a pull backward of water on the lens. For WindCubes there were less data to build up to the 10-min value during wipe. Very low aerosol concentrations may have resulted in lower data availability at the upper levels compared to lower levels but it was not often the case in the North Sea.

Table 4. The lidar deployment height and observational heights are listed in meter above mean sea level (AMSL). WC is WindCube, ZP is ZephIR.

Platform	Babbage	Beatrice	Fino3	HornsRev2	Jacky	ORP	Schooner	Siri	Taqa	Utsira
Lidar type	ZP	ZP	ZP	WC	WC	WC	WC	WC	WC	WC
Height	42	42.5	26	26	28	30	36	45	30	26
1	60	52.5	51	66	60	70	76	85	70	67
2	80	75.5	71	86	80	90	92	*105*	90	80
3	*100*	90.5	91	*106*	*100*	*110*	*99*	125	*110*	*100*
4	130	*105.5*	*101*	126	116	130	102	145	130	120
5	160		130	146	130	150	107	161	150	140
6			160	166	160	170	116	175	170	160
7				196	200	190	126	205	190	180
8				226	250	210	152	245	210	200
9				256	300	230	182	295	230	250
10				286			216	345	250	300

Table 5. System and data availability in % and hours are listed during the offshore deployment. The values are for observations at around 100 m AMSL.

Lidar	System Availability in %	Operational Hours	Data Availability in %	Data Hours
Utsira	85	14,995	81	12,075
Horns Rev 2	98	18,433	98	18,019
Taqa	99	9,120	97	8,870
Siri	95	9,585	85	8,178
Fino3	98	4,304	88	3,778
ORP	100	792	73	581
Jacky	97	5,622	93	5,228
Beatrice	86	9,597	85	8,154
Babbage	99	6,255	97	6,070
Schooner	86	8,583	76	6,538
Total		87,286		77,491

The carrier-to noise ratio (CNR) and availability for some WindCube lidars is shown in Figure 6. The observations show the lower signal with higher observational height due to weaker signal and mainly because of lower aerosol content at the higher heights. The maximum CNR is around 100 m or slightly below. The CNR behavior with height shows a peak because of the focus of the system [20].

The observations at Siri were similar in quality to the other instruments from June 2010 to 18 November 2010. After this time the lidar suffered from a still unknown issue preventing to record good data above its 40 m level during night time.

Figure 6. Lidar observations offshore from four lidars. (**a**) The carrier-to-noise ratio (CNR) as a function of observations height above installation. (**b**) The average data availability as a function of observations height above installation.

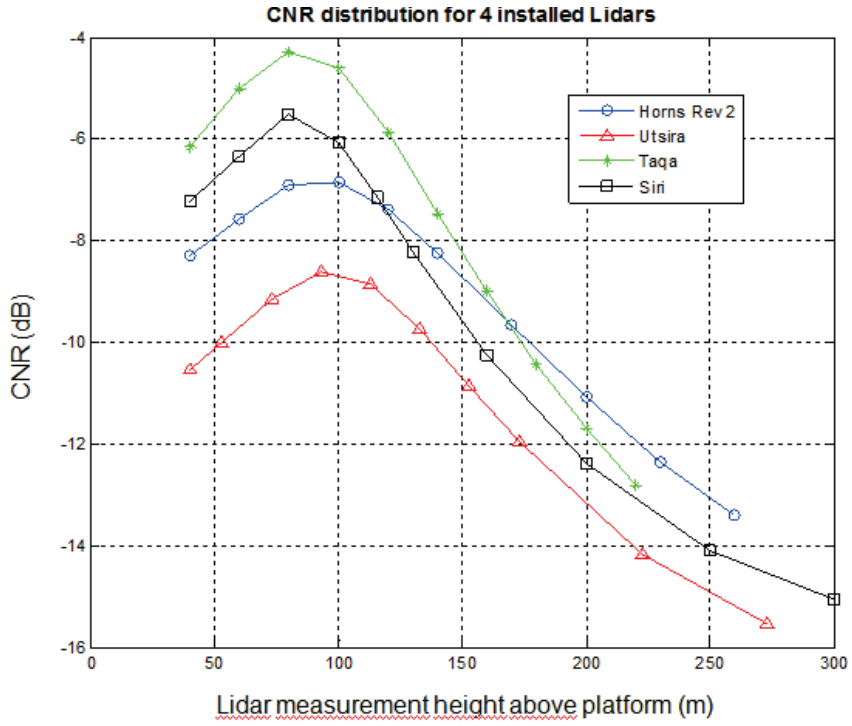

(**a**)

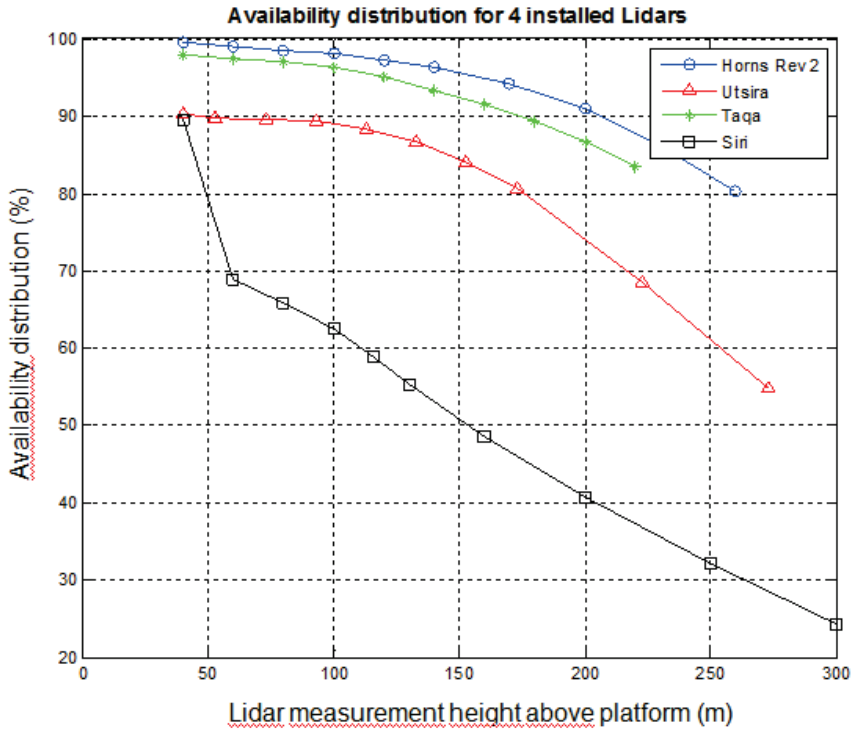

(**b**)

6. Flow Distortion due to Offshore Platform and Terrain

Nine of the lidars were deployed on offshore platforms. These platforms included large gas and oil drilling rigs with tall derrick structures (Beatrice, Siri, Taqa, ORP), smaller unmanned production

platforms (Jacky, Schooner, Babbage), wind farm transformer stations (Horns Rev 2 in the North Sea, Denmark) and a platform mounted meteorological mast (Fino3 in the North Sea, Germany). One lidar was deployed on the coast of the island of Utsira, see [8] for details. Common to all installations was the risk of flow distortion around the structures or influence from the surrounding landscape on the observed wind profile. The aim of the NORSEWInD project was to accurately observe free stream winds at hub height; thus it was desirable to minimize the flow distortion on the lidar wind profile observations by selecting the observational heights with care. In certain cases it could, however, become necessary to correct the wind profile observations.

To investigate the flow distortion around the platforms and to validate the Computational Fluid Dynamic (CFD) simulations, measurements in a low speed wind tunnel were made with a calibrated DANTEC Streamline constant temperature (CTA), triple wire anemometer mounted on a three dimensional traversing rig as shown in the diagram of Figure 7.

Figure 7. Diagram of constant temperature (CTA) probe traverse system showing the wind tunnel coordinate system and a plan view of wind tunnel layout.

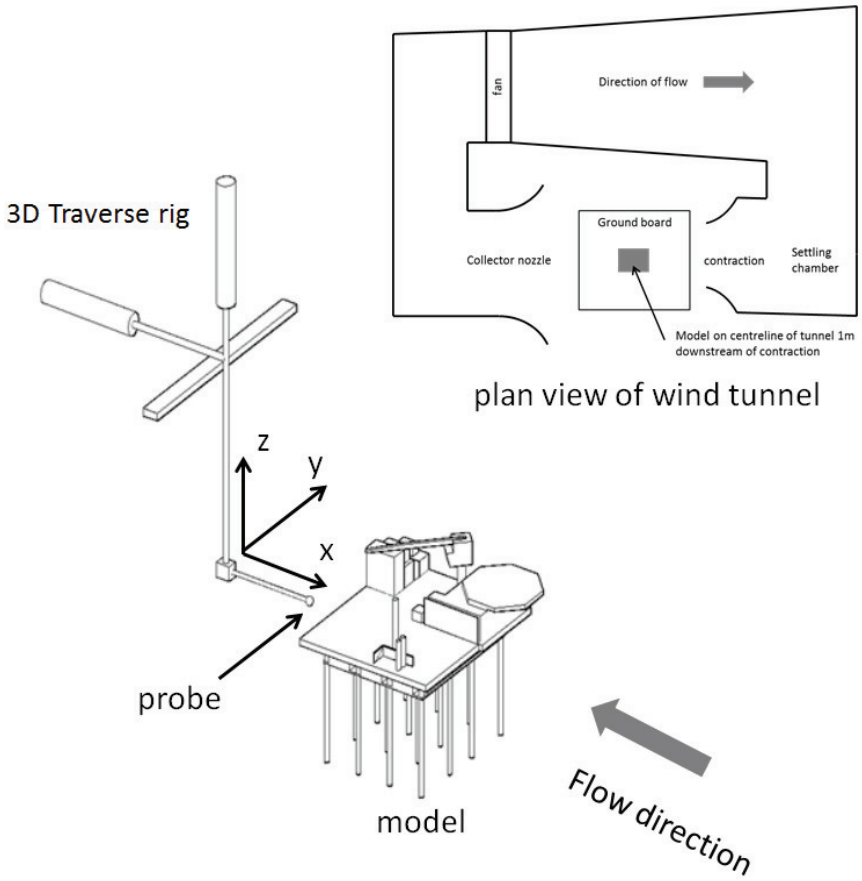

By traversing the hot wire probe vertically above the location of the simulated lidar the velocity profile in a vertical line above the rig could be determined. This velocity profile was then compared with the results of the CFD simulation of the rig. Initially, to create a base line against which the effect of the rig on the flow field could be assessed, the flow in the wind tunnel was traversed without the rig model present in the tunnel. The measured vectors were then non-dimensionalised by a reference wind speed measured by a single hot wire probe upstream and to the right of the proposed model location,

with due care taken to ensure the reference speed was outside any likely flow disturbance that might be caused by the presence of the rig model. This provided the non-dimensional, undisturbed, free stream velocity at the measurement locations above the rig for neutral conditions.

Simulations were undertaken at model scale and full scale to identify any issues regarding Reynolds number effects in the subscale wind tunnel tests and none were found. Length scale for oil production platforms was typically between 0.5 m and 1 m and 1.5 m for models of the island. Tunnel free stream speed was 15 $m \cdot s^{-1}$ in all cases. Platform models were typically 100th scale and 1,250th scale of the platforms and island, respectively. The CFD simulations were carried out for turbulent flow and the turbulence intensity in the 1.5 m low speed wind tunnel is approximately 1%. The k-omega turbulence model was selected because the model is a mature and established algorithm intended for general use with external flows [21]. To confirm the validity of the CFD simulation and to evaluate the most appropriate turbulence model the data collected by the hot wire traverses above the rig were compared to the CFD data at the same locations using a range of turbulence models including the k-ω and the standard k-ε model.

Figure 8. Non-dimensional velocity magnitude profiles measured above the platform with the flow approaching from four different azimuth angles.

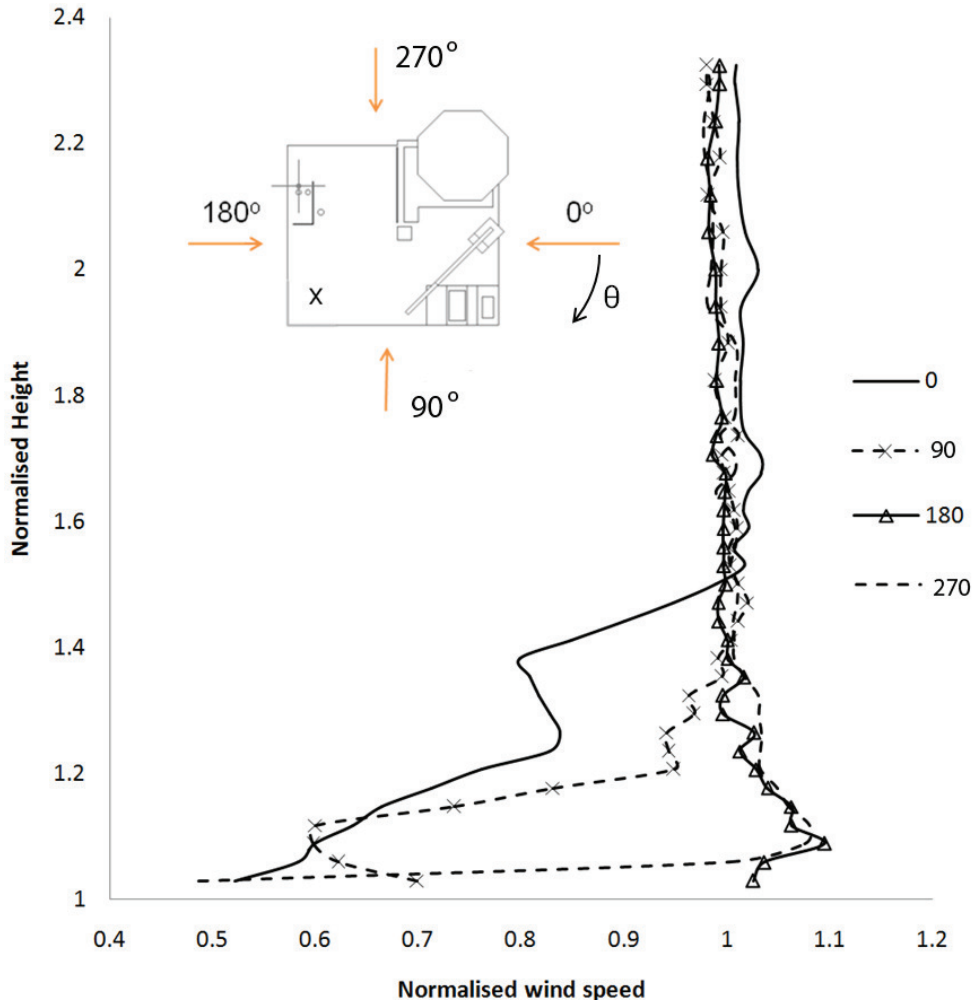

The rig was then placed in the tunnel and the velocity profiles above the rig measured. Comparing this data with the data acquired in the empty tunnel the effect of the presence of the rig on the undisturbed flow field was determined. Figure 8 shows the results of four traverses above a rig with the flow approaching the rig from different azimuthal angles. The X on the plan form view of the rig shows the location above which the probe was traversed in the positive Z direction. Probe heights were normalised by the height of the rig deck and the speed was normalised by the free stream velocity of the wind tunnel [22].

The data from the wind tunnel tests served two purposes: to assess the height above the platform that a point measurement device, such as a cup and vane anemometer, might be affected by flow distortion, and to verify CFD simulations which were required to assess the effect of flow distortion on the measurements made by lidars. By rotating the platform 360° in the wind tunnel and measuring the velocity profiles, the boundary where the flow velocity magnitude was within a certain percentage of the free stream velocity could be determined, see Figure 9. The result of this analysis for a number of platforms is shown in Table 6. The CFD model results compared well with the wind tunnel experiment [9,23] and were used to determine the effect of flow distortion on the measurements made by the lidars both onshore and offshore. The effect of flow distortion on the cup and vane type anemometer, being essentially a point measurement, is easily understood and measured. However, remote sensing devices, such as lidars and sodars, determine the wind vector from a spatially averaged set of measurements.

Figure 9. Height above rig required for 99% free stream velocity magnitude as a function of the azimuth angle from wind tunnel and Computational Fluid Dynamic model (CFD) results.

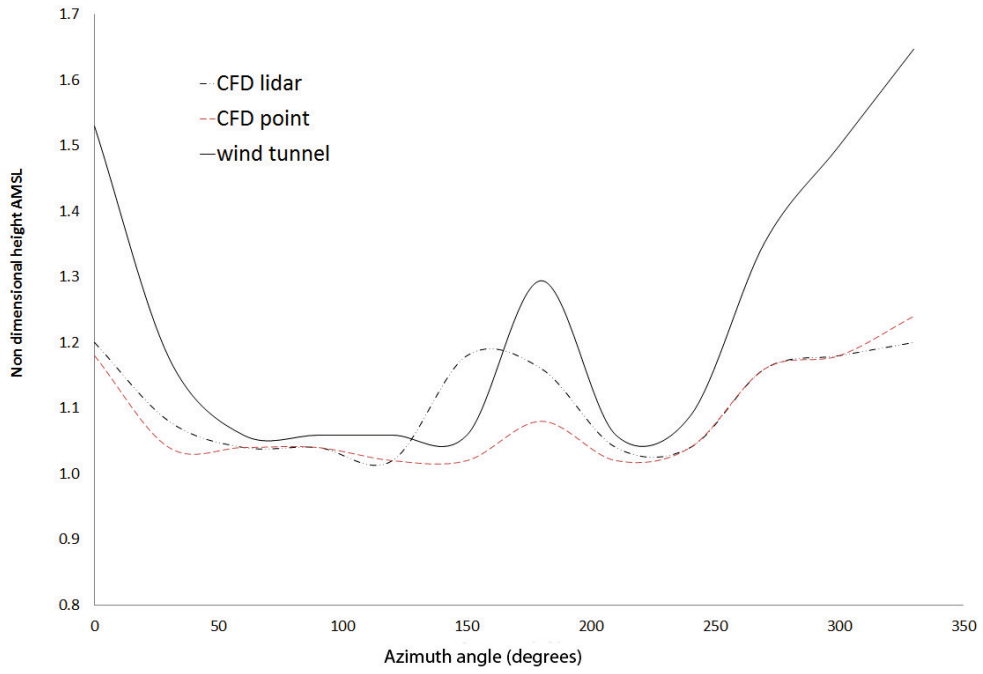

Some attempts have been made to measure the effect of flow distortion on lidars in complex terrain as might be found when measuring in hilly or mountainous terrain [2,5,19,24–27]. In the WAsP Engineering software [28], a program for wind site assessment, a script is available that accounts for the error due to the flow distortion created by orography when scanning conically with two types of

lidars [25]. The authors of [8] investigated the influence of the landscape to the wind profile observed by the lidar on the island of Utsira and found significant influence to the wind profile at all levels and with clear azimuthal dependence. However, the effect of the flow distortion on lidars in close proximity to large structures, such as buildings and oil rigs, had not been investigated to date. To understand the difficulty of estimating the effect of flow distortion on the measurements made by a lidar it is necessary to understand the fundamental difference between the point measurement of a cup anemometer and the spatially averaged velocity measurement of a lidar.

Table 6. Height above lidar installation level and AMSL for undisturbed flow measurement from wind tunnel and CFD point measurement and by lidar based simulation from CFD where u is the magnitude of the wind velocity and θ is flow angle in the horizontal plane. The values in the columns are height in meters AMSL at which this measurement is unaffected (±2.5% free-stream) by distortion. Numbers in brackets are the height at which distortion is negligible non-dimensionalised by the platform height.

			Height above Lidar in m (Height Normalized by Rig Height)					Height AMSL for 2.5% Free-Stream	
	Rign	Lidarm	Wind Tunnel	CFD Results				CFD Results	
Platform	Height	Height	Point	Point		Lidar		Lidar	
	(m)	(m)	u	u	θ	u	θ	u	θ
Babbage	42	42	33 (0.8)					75	
Beatrice	62	42.5	64 (1.0)	30 (0.5)	>64 (1.0)	34 (0.5)	59.5(1.0)	76.5	102
HornRev 2	26	26	30 (1.2)	44 (1.7)	57 (2.2)	25 (1.0)	55 (2.1)	50	80
Jacky	28	28		20 (0.7)	19 (0.7)	10 (0.4)	18 (0.6)	38	46
Schooner	38	36.25	24 (0.6)	24 (0.6)	35 (0.9)	9 (0.2)	24 (0.6)	39	54
Taqa	31.4	30	37 (1.2)	30 (1.0)	36 (1.1)	33 (1.1)	27 (0.9)	63	57
Utsira	26	26		108 (4.2)	192 (7.4)	150 (5.8)	300 (11.5)	176	326

The measurement technique employed by lidar systems relies on spatially averaged line of sight velocity measurements of the flow field. To measure a 3D velocity vector three or more line of sight velocity vectors are required. Depending on the instrument and the technique employed the number of line of sight vectors can be as low as 4 (WindCube) or as high as 150 (ZephIR). In order to assess the likely impact of an inhomogeneous flow field on such measurement techniques it was necessary to simulate more than a single point in the flow and assess any interference that might exist at each measurement point. Only when this interference at every measurement location had been found the effect on the final velocity vector could be determined.

To assess the effect of a platform's flow distortion on the lidars, the flow field over each platform was simulated using CFD and so the measurements performed by a scanning lidar. In this way the extent to which the platform affected the measurements made by a lidar mounted on that platform could be determined. The CFD data also provided information on the distortion observed by a point measurement device such as a cup anemometer.

As shown in Table 6 the height to which the platforms caused distortion was not the same. Horns Rev 2, a transformer platform, caused distortion in the magnitude of the velocity vector in the horizontal plane, U_{mag}, up to a height equivalent to that of the rig whereas Schooner created distortion

up to 0.2 times the rig height only. The extent to which distortion was created appeared to be a function of the solidity of the rig. The open lattice type structures created significantly less distortion than the more solid structures such as Horns Rev 2. It should be noted that the CFD simulations indicated that the lidar measurements were less susceptible to flow distortion than a point measurement at the same height. Also of note was the height to which the island of Utsira created distortion.

From the simulation of the lidar measurements in the distorted flow field it was possible to calculate correction factors and addends that could be applied to the data measured by the lidars situated on the offshore platforms. To correct the magnitude and direction of the free stream velocity vector in the horizontal plane, u and θ respectively, to the undisturbed free stream values Equations (1) and (2) were derived. In the simulation the values of u-free stream and θ-free stream in the undisturbed flow were known and the measurements made by a lidar, u-lidar and θ-lidar in the distorted flow field could be determined from the lidar simulation. Substituting these values into Equations (1) and (2) allowed the corrections, cff_u and cff_θ, to be determined.

$$u_{\text{free stream}} = \text{cff}_u \times u_{\text{lidar}} \quad (1)$$

$$\theta_{\text{free stream}} = \theta_{\text{lidar}} + \text{cff}_\theta \quad (2)$$

Correction factors were a function of height and free stream flow angle as shown in Figure 10. Flow corrections were only applied to data where the correction required was greater than 2.5%, for the flow magnitude and 0.5° for the flow direction as this was considered to be the limits of the accuracy of the CFD simulation data. Corrected and uncorrected data were stored separately in the database so that either version of the data could be analysed as required.

Figure 10. Correction added to the azimuth angle in the horizontal plane up to 50 m above rig height over 360° free stream azimuth flow angle in 30° steps.

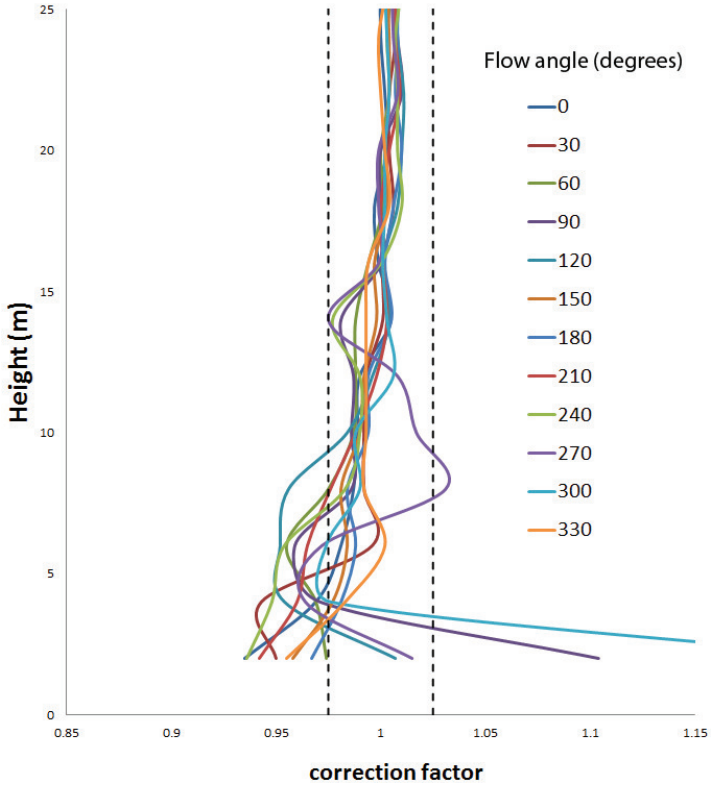

7. Database Architecture and Quality Control Implementation

The data from the lidar array was maintained on a Microsoft (MS) SQL Database Server. The database was stored on an externally attached high performance Dell RAID storage platform and backed up at regular scheduled intervals to disk and tape media. Data was transferred to the main database server via the standard File Transfer Protocol, either by manual transfer or automated scripting techniques. Upon successful transfer the data was then parsed onto the main MS SQL database. For reasons of security and data integrity, the MS SQL database was not directly accessible for data downloads or interrogation by end users. Secure database views determined by user ID were mirrored from the main MS SQL database to a separate MySQL database. This was accessed by user login ID and secured via an SSH connection through the University of Strathclyde's firewall, see Figure 11.

There were four tables of data within the database containing node definition, ZephIR, Windcube and meteorological mast data. Each lidar was assigned a node number against which information about the installation such as latitude and longitude of installation, installation height AMSL, type of device (ZephIR, Windcube, metmast), scan heights, filtering and verification, *etc*. was stored.

In order to upload data on to the database a user was required to log on to an FTP server with a node number specific login ID. Each node had a secure directory allocated and the user uploaded the data files into the relevant directory. A node specific login ID allowed access only to data belonging to that single node, access to additional node data was only allowed on the explicit instruction of the project coordinator or relevant node data owner.

Figure 11. Database structure and security implementation.

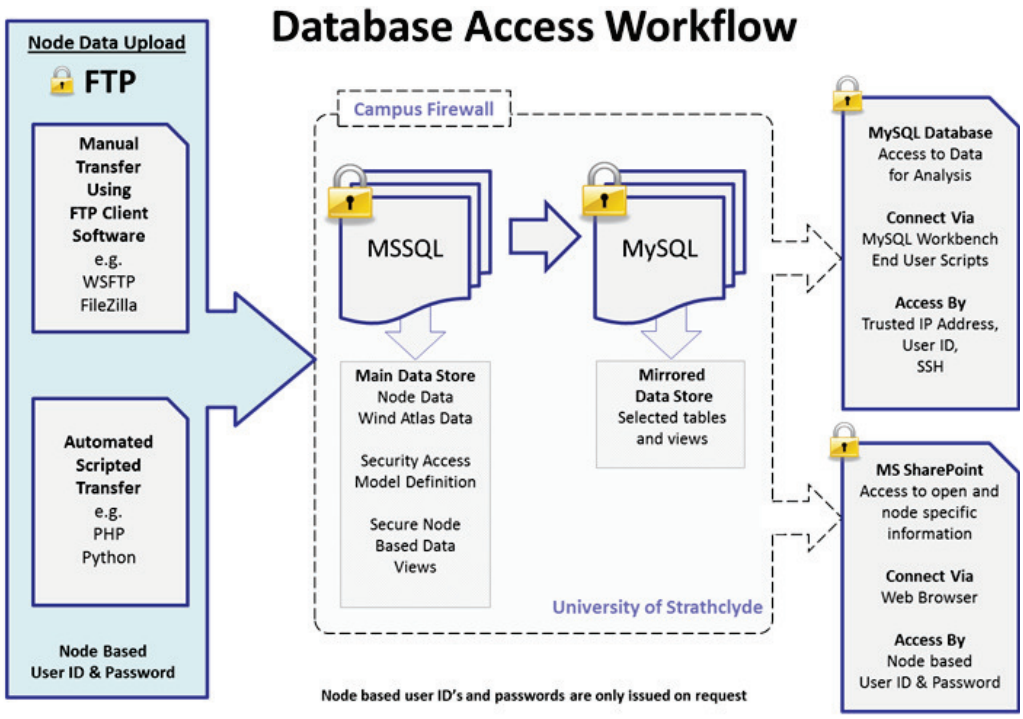

The SQL database created a transaction log (LogID) when data was uploaded and parsed into the database which contained node number, filename, login ID, and date and time of upload. This LogID

was used to tag the data for all future reference and allowed any single piece of data to be traced back to its original raw data file upload.

From the node number the format of the input data was known and the data was parsed into the data tables in a standard format for each lidar type. Data fields which contained data which signified poor data, such as 999,999, in the case of the Windcube, were replaced with null characters. Time and date stamping was also modified to follow the standard SQL date and time format.

Data integrity was checked by taking a random single time sequence of data or group of time sequenced data, and comparing the database data stored with the data sequence from the original uploaded raw CSV data file.

8. Selected Results of Hub Height Winds

One of the objectives of the NORSEWInD array of wind lidars was to evaluate the ability of numerical models to predict winds at hub height (~100 m) and, in particular, the vertical wind speed profile, since the final wind atlas was merely produced from the model outputs. Therefore, there was a need to compare the model results with observations on places where the wind resource at such levels had never been measured. Although most wind resource assessment software, such as the Wind Atlas Analysis and Application Program (WAsP) [29], estimate the wind turbine/farm energy production based on wind speed distributions at hub height and with that respect the outputs of a mesoscale model are rather good [30], the mesoscale models have shown difficulties to reproduce the wind profiles and, therefore, the vertical wind shear [31]. The latter becomes more important for wind turbines with large rotor areas as the difference between the below and above hub height winds might have a great impact on the loads and energy yield. Thus, we decided to concentrate on the analysis of the vertical wind shear observed by the wind lidars.

All NORSEWInD wind lidars were able to observe winds at 100 m and higher. Most of them were WindCube systems (Table 4), *i.e.*, pulsed lidars; thus the availability of data decreases with height (Figure 5). In order to maximize the amount of data we decided to estimate the wind shear from the two closest wind speed observations to the 100 m height. The wind shear is estimated as the value of the shear exponent α of the power law:

$$\frac{u_1}{u_2} = \left(\frac{z_1}{z_2}\right)^{\alpha} \tag{3}$$

where u is the magnitude of the wind speed, z the height, and 1 and 2 referred to two levels. α can then be estimated as:

$$\alpha = \frac{z}{u}\left(\frac{du}{dz}\right) \approx \frac{z}{u}\left(\frac{\Delta u}{\Delta z}\right) \tag{4}$$

Equation (4) is important because one can relate α to Monin-Obukhov similarity theory and will find that (see [8,32]):

$$\alpha = \frac{\Phi_m}{\ln\left(\frac{z}{z_0}\right) - \psi_m} \tag{5}$$

where z_0 is the surface roughness length and Φ_m is the dimensionless wind shear, which is a function of the dimensionless stability parameter z/L and also some sort of the derivative with respect to height of ψ_m and L is the Monin-Obukov length. Based on Equation (5), we therefore expect that within the

surface layer α is a function of height and will vary as z_0 increases with wind speed (among others) over the sea and ψ_m depends on the atmospheric condition. The relationship of α and stability was investigated from offshore mast data Fino-1 at heights below 80 m and compared to Large Eddy Simulation results [33] and the dependence of the power-law exponent on surface roughness and stability in a neutrally and stably stratified surface boundary layer was described by [34]. Recently [35] compared one year of lidar data to Fino-1 meteorological data, and [36] studied wind shear from the wind lidar observations at Fino-1 as a function of stability, and [37] compared data to meteorological data in upland terrain.

Figure 12 illustrates the distribution of α at a height close to 100 m, estimated using Equation (4), for all the NORSEWInD nodes where data is available in the database. The graph is based on 10-min observations from Beatrice (9034), Jacky (5347), Horns Rev 2 (94,848), Schooner (28,572), Siri (20,243), Taqa (47,317) and Utsira (59,908), the number of observations is given in brackets. There has not been any filtering related to the data in the sense that we have not used for example a minimum or maximum threshold of wind speed to be analyzed. The only filtering criteria used are related to the quality of the signals of the lidar; for the WindCubes the CNR and availability parameters and for the ZephIR we use the points of fit-figure, the degree of activity of the cloud correction algorithm and the precipitation signal, see [8]. If we start to look at particular conditions, the amount of data highly reduces. We need to maximize the amount of data for the analysis of the wind shear. As we have many pulsed lidars where the amount of data decreases with height, then we need to make a compromise between how much data we want to have and how high we want to observe. Since we want to see the shear at 100 m then we selected the two heights closest to it. Fitting a curve would bias the alpha estimation to the form of the fitted curve (the ideal will be to have two measurements very close to each other since alpha is in fact a very local parameter).

Figure 12. Normalized distribution of α-values from the power law at around 100 m for a number of NORSEWInD wind lidar nodes for all wind speed ranges.

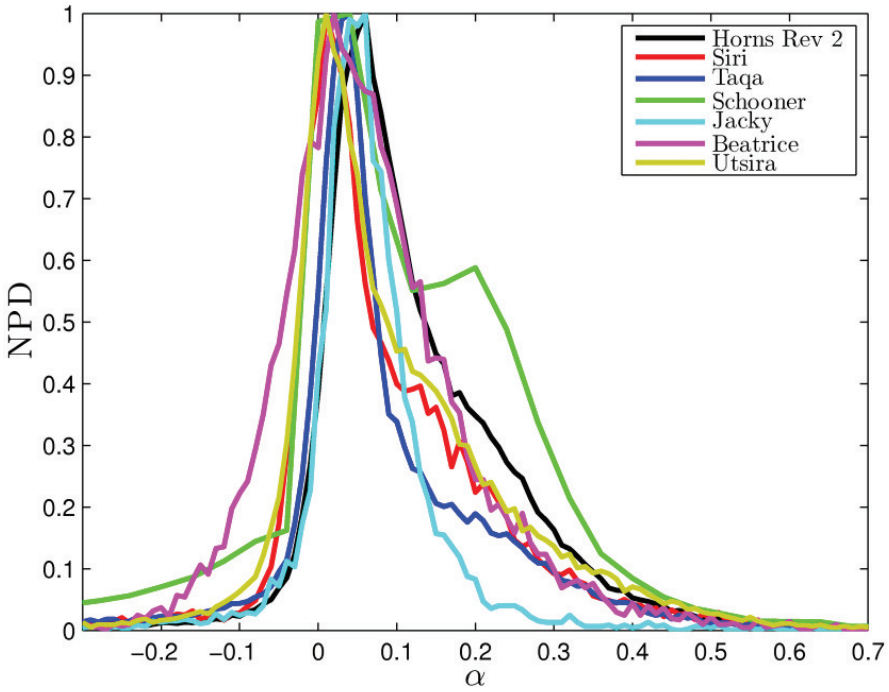

It is noticed that:

- For all the nodes, there is a broad range of α-values, mostly in the positive side of the distribution, which contrasts with the common value of 0.2 used for load calculations offshore. See [32] for further discussion of the α-value.
- A higher amount of positive α-values is found since wind speeds are generally higher above than below 100 m, as expected, but at all nodes it is also observed a good amount of negative α-values. The latter are normally found either under conditions where the atmosphere is very unstable and the wind speed does not change much with height (and so due to the nature of the atmosphere dynamics higher wind speeds are observed below 100 m) or conditions where the atmosphere is very stable and so low-level jets or shallow boundary layers influence the wind profile so that it bends backwards. It can straightforward be seen that predictions of the distribution of α using Equation (3) might only fit a range of positive values (no negative values can be estimated from it, although the conditions are very unstable and the sea roughness is high).
- Most distributions peak on a positive value between 0 and 0.05. The clearest exception is Horns Rev 2, which observes most of the time the wake of the wind farm that increases the wind shear at this particular height [8].
- Most distributions lie on each other; the greater exceptions are those at Jacky and Beatrice (the two with the fewest high-quality data for the analysis by far), and Schooner that shows a bump at about α = 0.2 which might not be real since we found a systematic problem with data, although the data here shown should be "correct" according to the NORSEWInD standards (see Table 1).

9. Discussions

The joint effort of the NORSEWInD team has resulted in new knowledge and lessons learnt in regard to observation of hub height wind measurements for wind energy using wind profiling lidars on offshore platforms and at the coast. The new knowledge includes three major issues on the device performance:

- The long term performance consistency for the wind profiling lidars employed is good. The so-called "NORSEWInD standard" pre-deployment validation showed excellent results for most of the lidars. Eight lidars were tested. The post-deployment validation tested four lidars and showed only minor deviations from the pre-deployment results. The results are very encouraging. They indicate that the devices have a high absolute accuracy after 6 to 26 months of deployment in the harsh offshore environment. Considering that the need for new bankable wind data for offshore wind farm projects is high wind profiling lidars appear to be a suitable candidate for this task in the future.
- The system consistency of the two types of lidars used is encouraging. There are several differences in two types of lidars including the number of observational levels, the difference in volumes of air observed and the sensitivity to cloud and fog, see [8] for further details. Despite the differences both types of lidars passed the "NORSEWInD standard" and had

similar post-deployment validation results. For winds at hub height both systems appear to perform well.

- The system availability for the devices when deployed offshore was lower than is typical on land. Offshore it ranged from 85% to 100% with an average of 95% but is typically higher at sites with better power supply. The data availability offshore ranged from 73% to 97% with an average of 89%. Data availability is typically higher at sites with higher aerosol concentration. System availability may be improved by providing better training to the rig personnel in operating and maintaining the devices. However, on some platforms there were no personnel. Otherwise it is recommended to improve the system reliability by the manufacturers designing future devices which require reduced operational care. Without some type of improvement on the system and data availability there is risk of insufficient long term observations necessary for accurate wind resource assessment when based on unmanned platforms offshore.

The new knowledge gained on flow distortion around the offshore platforms using both sub-scale models in a wind tunnel and CFD modeling indicates that the practical use of even rather bulky offshore structures is acceptable for observing free stream winds with lidars at hub height and below. A rough guide is that the flow is not significantly distorted above 2.4 times the deck height. It is clear that neither the wind tunnel experiments, nor CFD modeling is a final proof. It is therefore important to recognize that a critical analysis of the specific wind profiles observed on the platforms should always be performed in order to further verify that the wind information is trustworthy [8].

Although the hub heights and rotor diameters are growing, the lower tip height is not changing. This is fixed by the consenting authority and is usually in the order of 30 m AMSL. At this height it is unlikely a pulsed system (unless inclined and hence well outside potential flow distortion effects) will be able to acquire a signal. A cw system would be able to acquire a signal, however, if a larger host platform is used, then the observation would most likely be higher than the lowest tip height. In short we would not expect to correct for lower tip height values even using flow correction factors for wind lidar observations.

The major lessons learnt from the offshore deployment are technical and legal issues. In a research and demonstration project such as NORSEWInD legal issues with the platform owners took a while in several cases. However, it is the technical lessons learnt that will allow improved data collection for the future. So even with new generation lidars, for which several improvements were implemented, partly as a result of the experiences from NORSEWInD reported to the manufacturers, a device may need some care. The final wind observations are the 10-min mean values stored in the MySQL database. The aim of the NORSEWInD project was to observe offshore hub height winds for wind energy and to investigate the wind shear in the marine atmospheric boundary layer. It is easy to imagine many other research applications for which the observations could be useful. The data are available for research upon acceptance by the data owners (contact andy@oldbaumservices.uk for further information).

As discussed in [8] the wind profile lidar observations are stand-alone. No other types of observations are available from the platforms. Often information on air temperature, air temperature differences, humidity, boundary-layer height and other parameters are used for in-depth analysis of atmospheric boundary-layer behavior and structures. This is unfortunately not possible with this

dataset except if combined with other data sources such as numerical model results, satellite data or other sources as in [38,39].

10. Conclusions

The long-term performance consistency of wind profiling lidars used for offshore wind energy application has proven excellent. The devices operated offshore from around six months to more than two years. The so-called "NORSEWInD standard", where part of the criteria is that the slope of the linear regression should be within 0.98 and 1.01 and the linear correlation coefficient (R^2) should be >0.98 for the wind speed range 4–16 $m \cdot s^{-1}$, was used for the pre-deployment validation at Høvsøre comparing wind profiling lidar data to observation from a tall meteorological mast at 60, 80, 100 and 116 m. Five lidars passed the standard, two failed slightly whereas one device failed on several criteria. The post-deployment validation of four lidars showed excellent performance. The maintenance offshore was sparse but despite this and the harsh environment, the system availability was on average 95% out of a total of 127 months. The data availability was on average 89%. The system and data availability will have to be improved to obtain bankable offshore wind resource data. This is work for the future and most likely will be reached with a combination of improved devices and improved installation, operation and maintenance offshore.

The flow distortion on the offshore platforms was estimated to be insignificant for the lidar wind profile observations at hub height. Both CFD modeling and wind tunnel experiments with sub-scale models indicated this. The deployment of wind profiling lidars on large offshore structures appears suitable when the aim is to observe hub height winds at around 100 m AMSL. In contrast, the lidar wind data observed on the coast needed correction for the influence of the terrain as estimated by the flow model in WAsP Engineering and comparing the results to the lidar observations.

We were able to estimate the vertical wind shear distributions, based on the shear exponent of the power law, at several NORSEWInD wind lidar nodes and found a very broad range of values, peaking very close to zero, which contrasts with the commonly used constant value offshore of 0.2. This broad range of values is partly due to variation of the vertical wind shear with height, surface roughness (and thus sea state), and atmospheric stability, and partly to the atmosphere dynamics, which is not accounted for in many wind prediction models.

Acknowledgements

EU-NORSEWInD project funding TREN-FP7EN-219048 is acknowledged. Collaboration with DONG energy, Statoil Hydro ASA, TAQA, Shell UK, Talisman Energy, Kinsale Energy, Scottish Enterprise, Scottish and Southern Renewables, SSE and 3E is kindly acknowledged.

Conflicts of Interest

The authors declare no conflict of interest.

References

1. Wagner, R.; Antoniou, I.; Pedersen, S.M.; Courtney, M.S.; Jørgensen, H.E. The influence of the wind speed profile on wind turbine performance measurements. *Wind Energy* **2009**, *12*, 348–362.
2. Peña, A.; Hasager, C.B.; Gryning, S.; Courtney, M.; Antoniou, I.; Mikkelsen, T. Offshore wind profiling using Light Detection and Ranging Measurements. *Wind Energy* **2009**, *12*, 105–124.
3. Hahmann, A.N.; Lange, J.; Peña, A.; Hasager, C.B. *The NORSEWInD Numerical Wind Atlas for the South Baltic*; DTU Wind Energy E-0011 (EN); DTU Wind Energy: Roskilde, Denmark, 2012; p. 53.
4. Smith, D.A.; Harris, M.; Coffey, A.S.; Mikkelsen, T.; Jorgensen, H.E.; Mann, J.; Danielian, G. Wind lidar evaluation at the danish wind test site in hovsore. *Wind Energy* **2006**, *9*, 87–93.
5. Kindler, D.; Oldroyd, A.; Macaskill, A.; Finch, D. An eight month test campaign of the Qinetiq ZephIR system: Preliminary results. *Meteorol. Z.* **2007**, *16*, 479–489.
6. Antoniou, I.; Jørgensen, H.E.; Mikkelsen, T.; Frandsen, S.; Barthelmie, R.; Perstrup, C.; Hurtig, M. Offshore Wind Profile Measurements from Remote Sensing Instruments. In Proceedings of the European Wind Energy Association Conference & Exhibition in Athens, Athens, Greece, 27 February–3 March 2006.
7. NORSEWInD. Available online: http://www.norsewind.eu (accessed on 3 September 2013).
8. Peña, A.; Mikkelsen, T.; Gryning, S.-E.; Hasager, C.B.; Hahmann, A.; Badger, M.; Karagali, I.; Courtney, M. *Offshore Vertical Wind Shear: Final Report on NORSEWInD's Work Task 3.1*; DTU Wind Energy-E-Report-0005(EN); DTU Wind Energy: Roskilde, Denmark, 2012; p. 116.
9. Stickland, M.; Scanlon, T.; Fabre, S.; Oldroyd, A.; Mikkelsen, T. Measurement and simulation of the flow field around a triangular lattice meteorological mast. *J. Energy Power Eng.* **2013**, submitted.
10. Badger, M.; Badger, J.; Nielsen, M.; Hasager, C.B.; Peña, A. Wind class sampling of satellite SAR imagery for offshore wind resource mapping. *J. Appl. Meteorol. Climatol.* **2010**, *49*, 2474–2491.
11. Berge, E.; Hasager, C.B.; Bredesen, R.E.; Hahmann, A.; Byrkjedal, O.; Peña, A.; Kravik, R.; Harstveit, K.; Costa, P.; Oldroyd, A. NORSEWIND—Mesoscale Model Derived Wind Atlases for the Irish Sea, the North Sea and the Baltic Sea. In European Wind Energy Association Confernce, Vienna, Austria, 4–7 February 2013; pp. 1–6.
12. Hasager, C.B.; Badger, M.; Peña, A.; Larsen, X.G.; Bingol, F. SAR-Based wind resource statistics in the Baltic Sea. *Remote Sens.* **2011**, *3*, 117–144.
13. Karagali, I.; Hoyer, J.; Hasager, C. SST diurnal variability in the North Sea and the Baltic Sea. *Remote Sens. Environ.* **2012**, *121*, 159–170.
14. Karagali, I.; Peña, A.; Badger, M.; Hasager, C. Wind characteristics in the North and Baltic Seas from the QuikSCAT satellite. *Wind Energy* **2012**, doi: 10.1002/we.1565.
15. Karagali, I.; Badger, M.; Hahmann, A.; Peña, A.; Hasager, C.; Sempreviva, A.M. Spatial and temporal variability in winds in the Northern European Seas. *Renew. Energy* **2013**, *57*, 200–210.
16. ZephIR©. Available online: http://www.zephirlidar.com (accessed on 3 September 2013).
17. Pitter, M.; Slinger, C.; Harris, M. Introduction of Continous-Wave Doppler Lidar. In *Remote Sensing for Wind Energy*; Peña, A., Hasager, C.B., Lange, J., Anger, J., Badger, M., Bingöl, F., Bischoff, O., Cariou, J.-P., Dunne, F., Emeis, S., *et al*., Eds.; DTU Wind Energy-E-Report-0029(EN); DTU Wind Energy: Roskilde, Denmark, 2013; pp. 72–103.

18. WindCube©. Available online: http://www.leosphere.com (accessed on 3 September 2013).
19. Cariou, J.-P. Pulsed Lidars. In *Remote Sensing for Wind Energy*; Peña, A., Hasager, C.B., Lange, J., Anger, J., Badger, M., Bingöl, F., Bischoff, O., Cariou, J.-P., Dunne, F., Emeis, S., *et al*., Eds.; DTU Wind Energy-E-Report-0029(EN); DTU Wind Energy: Roskilde, Denmark, 2013; pp. 104–121.
20. Sonnenschein, C.M.; Horrigan, F.A. Signal-to-Noise relationships for Coaxial Systems that heterodyne backscatter from atmosphere. *Appl. Opt.* **1971**, *10*, 1600–1604.
21. Menter F.R.; Kuntz M.; Langtry, R. Ten Years of Industrial Experience with the SST Turbulence Model. In *Turbulence, Heat and Mass Transfer 4*; Hanjalic, K., Nagano, Y., Tummers, M., Eds.; Begell House Inc.: New York, NY, USA, 2003; pp. 625–632.
22. Courtney, M.; Wagner, R.; Lindelöw, P. Testing and comparison of Lidars for profile and turbulence measurements in wind energy. *IOP Conf. Ser.: Earth Environ. Sci.* **2008**, *1*, 012021, doi:10.1088/1755-1315/1/1/012021.
23. Stickland, M.; Scanlon, T.; Fabre, S. Computational and Experimental Study on the Effect of Flow Field Distortion on the Accuracy of the Measurements made by Anemometers on the Fino3 Meteorological Mast. In Proceedings of EWEA Offshore: Moving Ahead of the Energy Curve, Amsterdam, The Netherlands, 29 November–1 December 2011.
24. Bingöl, F.; Mann, J.; Foussekis, D. Conically scanning lidar error in complex terrain. *Meteorol. Z.* **2009**, *18*, 189–195.
25. Bingöl, F.; Mann, J.; Foussekis, D. Lidar error estimation with WAsP engineering. *IOP Conf. Ser.: Earth Environ. Sci.* **2008**, *1*, 012058, doi:10.1088/1755-1307/1/1/012058.
26. Bradley, S.; Mikkelsen, T. LIDAR remote sensing. *Int. Sustain. Energy Rev.* **2011**, *5*, 2–7.
27. Bradley, S.; Perrott, Y.; Behrens, P.; Oldroyd, A. Corrections for wind-speed errors from sodar and lidar in complex terrain. *Bound. Layer Meteorol.* **2012**, *143*, 37–48.
28. Mann, J.; Ott, S.; Jørgensen, B.H.; Frank, H.P. *WAsP Engineering 2000*; Technical Report Risø-R-1356(EN); Risø National Laboratory for Sustainable Energy, Technical University of Denmark: Roskilde, Denmark, 2002; Volume R–1356(EN), p. 101.
29. Mortensen, N.G.; Heathfield, D.N.; Myllerup, L.; Landberg, L.; Rathmann, O. *Getting Started with WAsP 9*; Report Risø-I-2571(EN) ; Risø National Laboratory for Sustainable Energy, Technical University of Denmark: Roskilde, Denmark, 2007; p. 72.
30. Peña, A.; Hahmann, A.; Hasager, C.B.; Bingöl, F.; Karagali, I.; Badger, J.; Badger, M.; Clausen, N. *South Baltic Wind Atlas*; Report Risø-R-1775(EN); Risø National Laboratory for Sustainable Energy, Technical University of Denmark: Roskilde, Denmark, 2011; p. 66.
31. Draxl, C.; Hahmann, A.N.; Peña, A.; Giebel, G. Evaluating winds and vertical wind shear from weather research and forecasting model forecasts using seven planetary boundary layer schemes. *Wind Energy* 2012, doi: 10.1002/we.1555
32. Emeis, S. Wind Energy Meteorology—Atmospheric Physics for Wind Power Generation. In *Series: Green Energy and Technology*; Springer: Heidelberg, Germany, 2012; p. 14–196.
33. Cañadillas, B.; Neumann, T.; Raasch, S. Getting a Better Understanding of the Offshore Marine Boundary Layer: Comparison between Large Eddy Simulation and Offshore Measurement Data with Focus on Wind Energy Application. In Proceedings of the Fifth International Symposium on Computational Wind Engineering (CWE2010), Chapel Hill, NC, USA, 23–27 May 2010.

34. Zoumakis, N.M. The dependence of the power-law exponent on surface roughness and stability in a neutrally and stably stratified surface boundary layer. *Atmósfera* **1993**, *6*, 79–83.
35. Westerhellweg, A.; Cañadillas, B.; Beeken, A.; Neumann, T. One Year of Lidar Measurements at FINO1-Platform: Comparison and Verification to Met-Mast Data. In Proceedings of 10th German Wind Energy Conference DEWEK 2010, Bremen, Germany, 17–18 November 2010.
36. Muñoz-Esparza, D.; Canadillas, B.; Neumann, T.; van Beeck, J. Turbulent fluxes, stability and shear in the offshore environment: Mesoscale modelling and field observations at FINO1. *J. Renew. Sustain. Energy* **2012**, *4*, 063136:1–063136:16.
37. Lang, S.; McKeogh, E. LIDAR and SODAR measurements of wind speed and direction in upland terrain for wind energy purposes. *Remote Sens.* **2011**, *3*, 1871–1901.
38. Takeyama, Y.; Ohsawa, T.; Yamashita, T.; Kozai, K.; Muto, Y.; Baba, Y.; Kawaguchi, K. Estimation of offshore wind resources in coastal waters off Shirahama using ENVISAT ASAR images. *Remote Sens.* **2013**, *5*, 283–2897.
39. Takeyama, Y.; Ohsawa, T.; Kozai, K.; Hasager, C.B.; Badger, M. Effectiveness of WRF wind direction for retrieving coastal sea surface wind from synthetic aperture radar. *Wind Energy* **2012**, doi: 10.1002/we.1526.

© 2013 by the authors; licensee MDPI, Basel, Switzerland. This article is an open access article distributed under the terms and conditions of the Creative Commons Attribution license (http://creativecommons.org/licenses/by/3.0/).